Neurochemical Research, Vol. 28, No. 1, January 2003 (© 2003), pp. 29–43

Spatiotemporal Distribution of the Insulin-Like Growth Factor Receptor in the Rat Olfactory Bulb*

Carina C. Ferrari,[1,2] Brett A. Johnson,[3] Michael Leon,[3] and Sarah K. Pixley[1,4]

(Accepted June 10, 2002)

Insulin-like growth factor I (IGF-I) and its receptor (IGF-IR) are involved in growth of neurons. In the rat olfactory epithelium, we previously showed IGF-IR immunostaining in subsets of olfactory receptor neurons. We now report that IGF-IR staining was heaviest in the olfactory nerve layer of the rat olfactory bulb at embryonic days 18, and 19 and postnatal day 1, with labeling of protoglomeruli. In the adult, only a few glomeruli were IGF-IR-positive, some of which were unusually small and strongly labeled. Some IGF-IR-positive fibers penetrated deeper into the external plexiform layer, even in adults. In developing tissues, IGF-IR staining co-localized with that for olfactory marker protein and growth associated protein GAP-43, but to a lesser extent with synaptophysin. In the adult, IGF-IR-positive fibers were compartmentalized within glomeruli. IGF-I may play a role in glomerular synaptogenesis and/or plasticity, possibly contributing to development of coding patterns for odor detection or identification.

KEY WORDS: Olfactory bulb; IGF-IR; olfactory marker protein; synaptophysin; growth-associated protein; confocal microscopy.

INTRODUCTION

Insulin-like growth factor I (IGF-I) is a peptide involved in growth and development of several mammalian cell types, including neurons (1). In culture studies, IGF-I supports neuroblast cell division (2,3), neuronal survival (4–6), prevention of apoptosis (7–9), and neuronal differentiation (5,10–14). In the intact animal, IGF-I plays a role in both the developing and injured brain, regulating neuronal growth and differentiation, as well as preventing apoptosis (15,16). In fact, administration of IGF-I to intact animals increases cell proliferation and neurogenesis in the adult rat hippocampus (17). The specific role of IGF-I in the brain remains mysterious, although recent studies have proposed a convincing argument for its involvement in brain glucose metabolism (18).

During CNS development, IGF-I mRNA is expressed at unusually high levels in the projection neurons of the cerebellum and several ascending sensory systems, including the olfactory system (19). The mRNA for the IGF-IR, which is a membrane-bound tyrosine kinase homologous to the insulin receptor (20), is also expressed at high levels by these large projection neurons and some of the local neighboring interneurons in the olfactory bulb (OB) (19). The expression of high levels of IGF-I and IGF-IR mRNAs is transient in most neurons during development, but is retained in OB neurons throughout adult life. These expression patterns and timing suggested the hypothesis

* Special issue dedicated to Dr. Jean de Vellis.

[1] Department of Cell Biology, Neurobiology and Anatomy, University Cincinnati College of Medicine, Cincinnati, Ohio.
[2] Institute for Biochemical Research-Leloir Foundation, University of Buenos Aires-CONICET, Buenos Aires, Argentina.
[3] Department of Neurobiology and Behavior, University of California, Irvine, California.
[4] Address reprint requests to: Sarah K. Pixley, Department of Cell Biology, Neurobiology and Anatomy, Vontz Center for Molecular Studies (3125 Eden Avenue), University of Cincinatti College of Medicine, P.O. Box 670521, Cincinnati, Ohio 45267-0521. Tel: 513-558-6086; Fax: 513-558-4454; E-mail: sarah.pixley@uc.edu

0364-3190/03/0100–0029/0

that IGF-I was involved in the maturation of axonal connections, particularly synaptogenesis (19). The continued expression in the OB further supports this because synaptogenesis occurs throughout life in the OB (21,22).

Although the distribution of IGF-I mRNA in the OB suggests local autocrine and/or paracrine actions, the cells expressing IGF-I could also influence the peripheral olfactory receptor neurons (ORNs). Previous studies on the olfactory system suggested the hypothesis that the OB provides trophic support for maturation of ORNs, in particular for the survival of mature ORNs (23). We wondered if IGF-I might provide at least some of this trophic support. Recent studies in our laboratory have shown that insulin and IGF-I provide significant survival support for ORNs in culture (24). And immunoreactivity for the IGF-IR protein is present in a subset of immature ORNs in the peripheral OE (25). Therefore, to further explore the significance of IGF-I in the olfactory system, we investigated the distribution of IGF-IR immunoreactive (IGF-IR-positive, IGF-IR+) axons of ORNs in the OB in both the adult and during development.

The axons of ORNs terminate in neuropil-rich areas of the OB called glomeruli, which are sites of sophisticated information processing concerning detection and identification of odorants (26–28). Functional data show that individual glomeruli process information concerning either a single or very small number of odorant molecular features (29,30). Each glomerulus is the site of convergence of a much larger number of partially stochastically distributed ORNs that individually express one odorant receptor gene (26–28). The mechanisms of how ORN axons converge on glomeruli and of how odorant information is coded in the glomeruli are only partially understood and are areas of intense interest at present.

Knowledge about how glomeruli are organized, and how this organization arises during development and is then maintained in the face of constant renewal of ORNs, could illuminate how odorant coding is established. Previous ultrastructural studies have shown that glomerular formation, including formation of the first synaptic contacts, is initiated around embryonic day 16–18 in the rat, when incoming ORN axons and OB dendrites begin to form "protoglomeruli" (31). True glomeruli are identified first at 1 day after birth (32), and mature glomerular organization is evident by postnatal day 10 (31,33). However, given that the ORNs are continually replaced on a constant turnover basis throughout adult life (21,22), the glomeruli will always show continual synaptic plasticity.

The mechanisms underlying glomerular development and/or glomerular plasticity in mammals remain largely obscure. Recent studies have provided insights as to some of the spatiotemporal cellular interactions that occur during glomerular formation in embryonic (32) and postnatal mammalian development (34). And several types of molecules have been implicated in guidance of ORN axons and therefore possibly formation of glomerular contacts. These include extracellular matrix molecules (35–37), cell adhesion molecules (38–40), and odorant receptor proteins (28). However, many mysteries still remain and there has been no consideration or hint previously that growth factors might be involved in these processes.

To investigate the interesting possibility that IGF-I might be involved in glomerular patterning, we analyzed the spatiotemporal distribution of IGF-IRs on ORN axons in the OB. We also compared the pattern of IGF-IR immunoreactivity in the OB with that observed with antibodies against the olfactory marker protein (OMP), which labels almost exclusively mature ORN axons (41), the growth-associated protein GAP-43, which labels immature ORNs prior to the expression of OMP (42), and synaptophysin (SYN), an integral membrane protein of synaptic vesicles (43), which identifies the location of synapses. These studies have allowed us to characterize the pattern of IGF-IR protein expression during OB development from perinatal through adult stages.

EXPERIMENTAL PROCEDURE

Animals were handled following protocols approved by the University of Cincinnati and University of California at Irvine Animal Care and Use Committees, and that were in accordance with NIH guidelines for animal use. To obtain embryonic tissues, timed-pregnant rats were deeply anesthetized with sodium pentobarbital (65 mg/kg) and embryos were removed by cesarean section. Postnatal day 1 pups (prior to establishment of thermoregulation) were anesthetized with cold. Animals were killed by decapitation, and OB tissues were removed and placed in 4% paraformaldehyde in 0.1 M phosphate buffer (PB) overnight at 4°C. Adult rats (postpubertal females ~200–300 g) were anesthetized with sodium pentobarbital (65 mg/kg), perfused via the aorta with cold physiological saline followed by cold 4% paraformaldehyde for 30 min and decapitated. OB tissues were removed, fixed in the same fixative overnight at 4°C, and decalcified by immersion in a rapid decalcifying solution (RDO; Apex Engineering Products Corporation, Plainfield, IL) overnight at room temperature. All tissues were cryoprotected by immersion overnight in 20% sucrose in PB, embedded in M-1 embedding matrix (Lipshaw, Pittsburgh, PA), frozen by immersion in isopentane cooled with liquid nitrogen or ethanol/dry ice, and serially sectioned (15 μm) in a cryostat. Sections were mounted on Superfrost slides (Fisher, Cincinnati, OH), air-dried, and stored at −20°C until needed. The P20 rats (mixed sexes) were anesthetized (as for adults,

above) and decapitated, and OB tissues were removed and immediately frozen (as above). Serial sections were cut coronally at a thickness of 20 μm on a cryostat and collected on gelatin-subbed slides. No qualitative differences in IGF-IR staining were observed between fixed and P20 unfixed tissues.

For immunoperoxidase staining, frozen sections were air-dried for 20 min, incubated in blocking buffer (phosphate buffered saline (PBS) with 0.2% Triton X-100, 0.02% sodium azide and 2% goat serum) and then in the primary antibody, chicken anti-IGF-IR (1:100; Upstate Biotechnology, Lake Placid, NY) overnight at room temperature. The sections were then incubated in biotinylated goat anti-chicken (1:100; Vector Laboratories, Burlingame, CA) followed by an avidin-biotin–horseradish peroxidase complex (1:100 in PB; Vectastain Elite ABC reagent, Vector Laboratories). Incubations were for 2 hs at room temperature, antibodies were diluted in PBS with 0.2% Triton and 0.02% sodium azide, and rinses were in PBS or PB. Label was visualized with diaminobenzidine (DAB; 0.5 mg/ml in PB) and H_2O_2. Some alternate sections were stained with cresyl violet. The sections were dehydrated in graded alcohols, cleared in Hemo-De, and mounted in DPX. Light microscopy images were viewed on a Nikon FX microscope, digitalized using a Spot CCD Camera (Diagnostic Instruments), and labeled and arranged using Adobe PhotoShop 5.0.

For double immunofluorescence labeling, adjacent sections from rostral, middle, and caudal regions of the OB of each animal were chosen. Frozen sections were air-dried for 20 min, rinsed with PBS with 0.1% Triton (PBS-TX), and incubated in blocking buffer (PB with 0.5% rabbit serum and 0.1% Triton) for 45 min. Sections were then incubated overnight at room temperature in primary antibody combinations of anti-IGF-IR (1:50) and (i) anti-OMP (1:500; goat serum; gift of F. Margolis), (ii) anti-SYN (1:10: mouse monoclonal; Boehringer Mannheim Biochemical, now Roche Diagnostics, Indianapolis, IN), or (iii) anti-GAP-43 (1:20; mouse monoclonal; Boehringer Manheim Biochemical). After rinsing in PBS-TX, the sections were incubated for 1 h at room temperature in secondary antibody combinations of Cy5 conjugated rabbit anti-chicken (1:200; Jackson ImmunoResearch Laboratories Inc, West Grove, PA) and, respectively, (i) Alexa 488 conjugated rabbit anti-goat (1:200; Molecular Probes, Eugene, OR), (ii) Alexa 488 conjugated rabbit anti mouse (1:200; Molecular Probes), or (iii) Alexa 488 conjugated rabbit anti-mouse. Labeled sections were rinsed with PBS and mounted in Gelvatol (44). Digital images were collected from a Zeiss LSM510 laser scanning confocal microscope equipped with a krypton-argon laser and labeled and arranged with Adobe PhotoShop 5.0. Any materials not noted were from Sigma (St. Louis, MO) or Fisher Scientific (Cincinnati, OH).

RESULTS

Distribution of IGF-IR. To examine critical development periods in the morphological development of glomeruli (31,39), we analyzed IGF-IR immunostaining in serial sections of E18, E19, P1, young adult (P20), and adult OBs. We describe the embryonic regions of the OB according to previous reports (32).

At E18, IGF-IR+ fibers were found throughout the olfactory nerve layer (ONL), the most exterior layer of the OB (Fig. 1A). Some positive fibers extended into the dendritic zone (DZ), which at this age includes essentially all other layers of the OB. Greater numbers of IGF-IR+ fibers were found within the DZ when sections were labeled with DAB, than with immunofluorescence, suggesting a lower sensitivity, in our hands, with the fluorescent secondaries.

At E19, protoglomeruli were evident around the circumference of the OB with IGF-IR labeling (Fig. 1B, arrows). Protoglomeruli were not as uniform in shape or as distinctly separate from the ONL as mature glomeruli. IGF-IR reactivity was again observed throughout the ONL and extending into the protoglomeruli (Fig. 1B). The intensity of IGF-IR labeling was greater throughout the ONL than it was in the protoglomeruli, although this was more evident with fluorescence labeling.

At P1, when glomeruli become distinguishable, IGF-IR+ olfactory axons were again found as positive bundles or fibers interspersed with IGF-IR− axonal processes throughout the ONL (Fig. 1C). Some, but not all, glomeruli were IGF-IR+ (Fig. 1C, arrows). The IGF-IR+ glomeruli were more numerous than IGF-IR− glomeruli, and studies of the numbers and distribution within the OB are ongoing in the lab.

In the P20 and older rat OB, IGF-IR labeling was more restricted in distribution than at P1 (Fig. 2A–D for P20, 1D–E and Fig. 2E–G for adult rats). Older rats demonstrated fewer labeled glomeruli than P20 rats (compare Fig. 1D with 2A). In the rostral region of adult OBs, IGF-IR+ olfactory axons formed a nerve bundle that coursed caudally, staying in the most exterior portion of the ONL until the posterior bulb, where it formed the majority of the ONL. Other parts of the ONL in the anterior OB showed no IGF-IR labeling. In the middle and posterior OB, IGF-IR labeling of the ONL was more extensive, especially on the lateral and medial surfaces of the OB (Fig. 2A). Glomeruli beneath densely labeled areas of the ONL were not always all IGF-IR+, suggesting that many of the labeled fiber bundles were traveling to other areas of the OB.

Only a subset of glomeruli contained detectable IGF-IR+ fibers in the adult rat OB (see Fig. 1D, arrowhead). Interestingly, two types of IGF-IR+ glomeruli could be differentiated. The first type of glomeruli, which were most frequent, were larger and diffusely labeled (see Fig. 1E, arrowheads). At higher magnification, distinctly labeled fibers could not be identified. These glomeruli were much more common in the posterior bulb (Fig. 2A, C) than in the anterior bulb (n = 9 animals). In the ONL adjacent to these glomeruli, large bundles of IGF-IR+ olfactory nerves were observed that appeared to penetrate the glomeruli from the ONL. Fig-

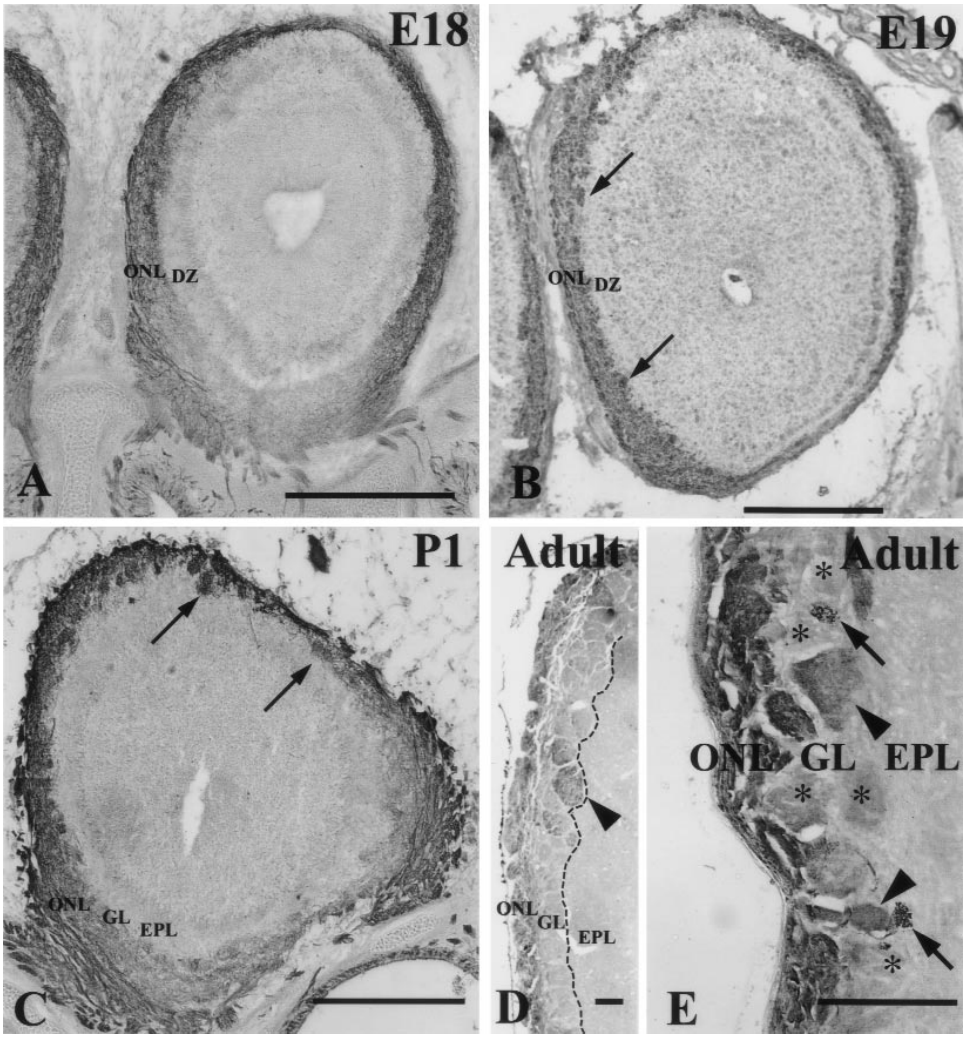

Fig. 1. Immunoperoxidase labeling for IGF-IR in transverse sections of the rat OB at different ages. **A,** Embryonic day 18 (E18): Most of the IGF-IR label was located in the ONL, but some IGF-IR+ fibers were observed in the DZ. Scale bar = 250 μm. **B,** Embryonic day 19 (E19): At E19 again most of the label was in the ONL. Protoglomeruli could be distinguished (arrows) in the DZ. Scale bar = 200 μm. **C,** Postnatal day 1 (P1): At P1 most of the staining was in the ONL, but IGF-IR+ glomeruli were also observed in the GL (arrows). Scale bar = 200 μm. **D,** Adult rat: In the adult (postpubertal) rat, only a few glomeruli were IGF-IR+ (arrowhead). Dotted line separates GL on the left from EPL on the right. Scale bar = 100 μm. **E,** Adult rat, higher magnification of a cluster of IGF-IR+ glomeruli. Glomeruli that are small and intensely labeled (arrows) can readily be distinguished from larger, less intensely and more diffusely labeled glomeruli (arrowheads). Asterisks indicate the position of glomeruli that were either negative or lightly labeled for IGF-IR. Scale bar = 200 μm. ONL, Olfactory nerve layer; DZ, dendritic zone; GL, glomerular layer; EPL, external plexiform layer.

ure 2A–D shows low- and high-magnification images of an IGF-IR stained section and a cresyl violet counterstained adjacent section from the posterior area of a P20 rat OB, anterior to the accessory OB. The arrows in Fig. 2A and B mark the boundary between labeled glomeruli dorsally and unlabeled glomeruli ventrally, which is better visualized in Fig. 2C–D. Some areas of staining appeared to be bilaterally symmetrical. The second type of glomerulus was unusually small, and labeling for IGF-IR was more intense (see Fig. 1E, arrows, and Fig. 2E–G). These smaller IGF-IR+ glomeruli were even less frequently seen than larger ones, and they were often located in the transitional region between the GL and EPL (see Fig. 1E, lower arrow). On closer inspection, the darkly labeled fibers in these glomeruli formed a loose network, followed tortuous courses, and appeared to have numerous varicose segments along their branches (see Fig. 1E, arrows, and Fig. 2E–G). Further investigation, including quantification and interanimal distribution patterns of both types of IGF-IR+ glomeruli, are currently ongoing in the lab.

In the postpubertal adult rats, IGF-IR+ fibers were also observed leaving glomeruli and penetrating deeper, into the EPL (Fig. 2F and arrows in 2E and

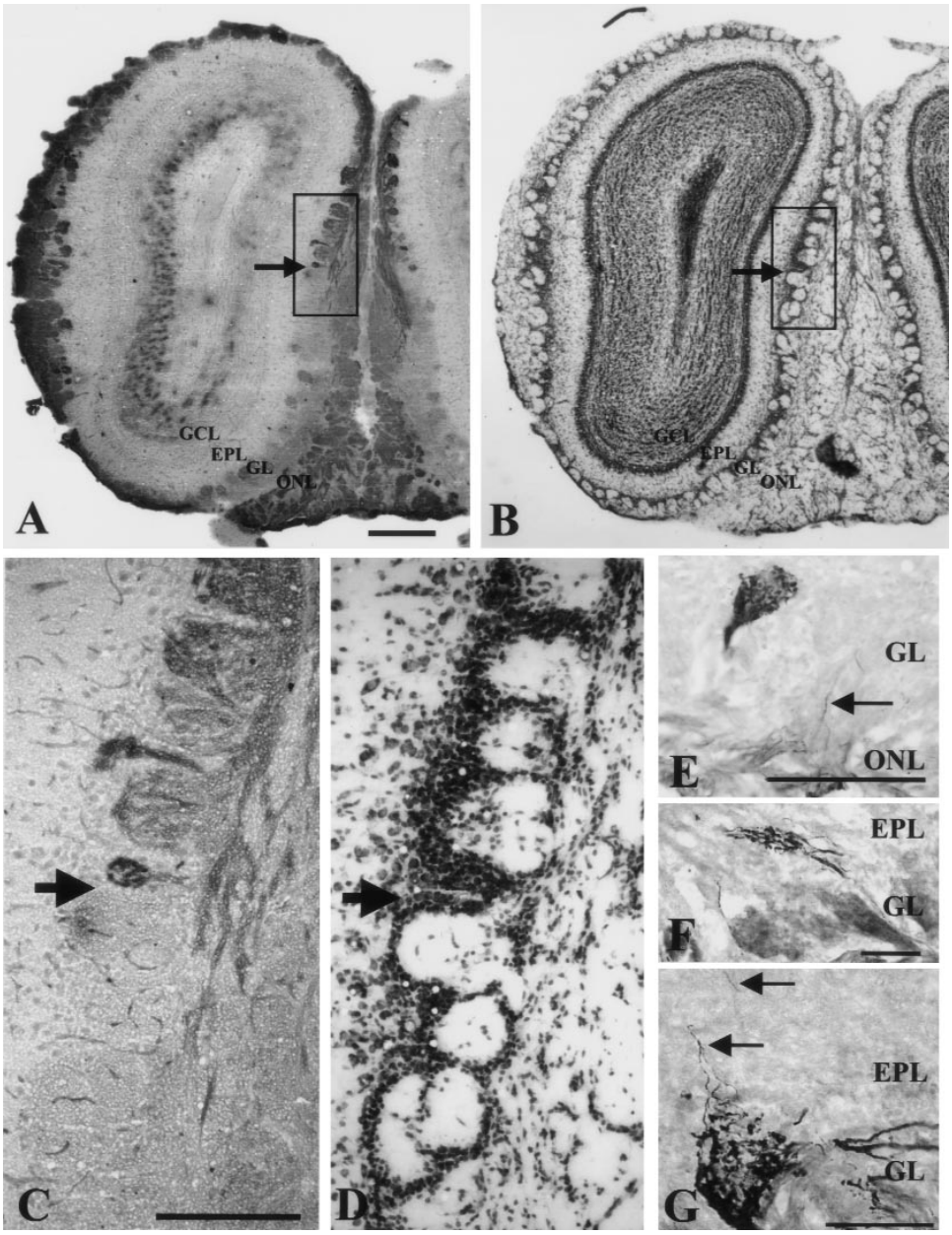

Fig. 2. Further details of anti-IGF-IR immunoperoxidase labeled OB sections. **A** and **B,** Adjacent serial OB sections from a P20 animal, labeled with anti-IGF-IR (**A**) or cresyl violet (**B**) (dorsal is to the top, medial to the left). Only certain glomeruli and areas of the ONL were labeled. Arrow indicates dividing line between densely labeled glomeruli (dorsal) and lightly labeled or negative glomeruli (ventral), along the medial surface. Scale bar = 500 μm. Box indicates areas shown at higher magnification in **C** and **D. C** and **D,** Close-up of the area including both labeled (above arrow) and unlabeled or lightly labeled (below arrow) glomeruli. Scale bar = 200 μm. **E, F, G,** Details of adult (postpubertal) rat OB sections labeled with anti-IGF-IR. **E,** Detail of a small, intensely IGF-IR+ glomerulus located adjacent to, if not in, the EPL (just internal to the GL). Some IGF-IR+ fibers (arrow) were observed penetrating into the GL. Scale bar = 200 μm. **F,** Another small glomerulus and IGF-IR+ fibers located in the EPL. Scale bar = 50 μm. **G,** A small and strongly stained glomerulus is shown at the transition between the GL and EPL, with IGF-IR+ fibers (arrows) penetrating into the EPL. Scale bar = 150 μm.

2G). The immunoreactive fibers were mostly located near IGF-IR+ glomeruli and were more numerous near the smallest and most strongly stained glomeruli. IGF-IR+ fibers penetrating into the EPL were also observed in younger animals (not shown).

Double-Labeling with OMP and IGF-IR. At E18, there was extensive co-localization between OMP and IGF-IR labeling, in both the ONL and DZ (Fig. 3A–C), suggesting that some IGF-IR+ fibers were mature ORN axons. However, this co-localization was not as com-

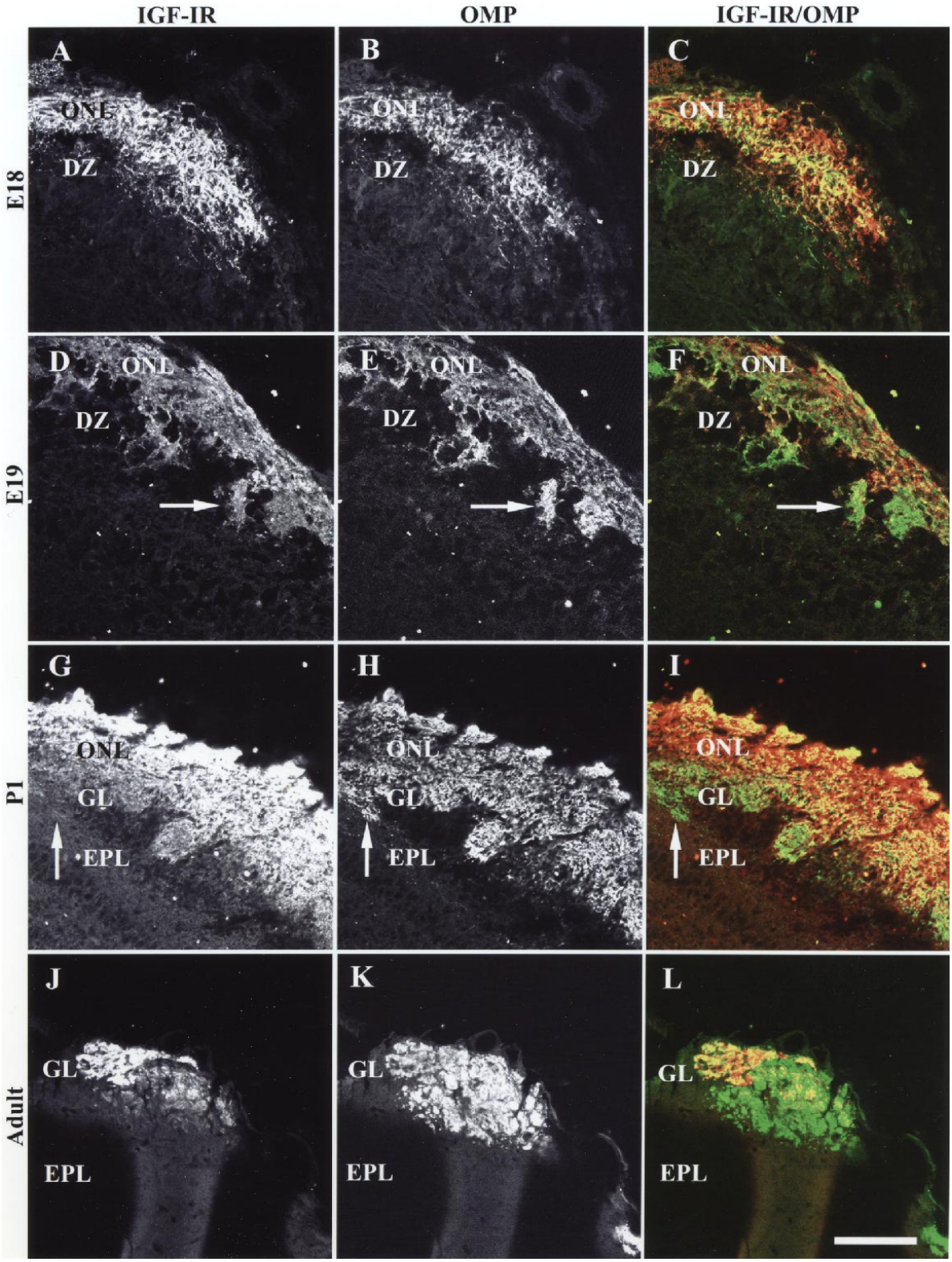

Fig. 3. Double immunofluorescence labeling: IGF-IR (red) and OMP (green). **A–C,** At E18, labeling for both IGF-IR (A) and OMP (B) was located primarily in the ONL. However, some double-labeled (IGF-IR+/OMP+) (yellow in C) fibers extended into the DZ. **D–F,** At E19, the ONL was again positive, with double-labeling also found in protoglomeruli (yellow, arrows). **G–I,** At P1, both markers were expressed mostly in the ONL, with some labeling of glomeruli (yellow). **J–L,** In the adult (postpubertal) rat, most of the glomeruli were positive only for OMP (green). However, within the glomeruli containing IGF-IR staining, some regions were double-labeled (yellow in L) and others were positive only for IGF-IR (J, red in L) or OMP (K, green in L). Scale bar (for all) = 100 μm. A color version of this figure can be viewed in the online version of the journal at http://www.kluweronline.com/issn/0364-3190.

plete as with GAP-43 (see below). Roughly 5–15% of IGF-IR+ fibers were OMP-negative, and approximately the same percentage of OMP+ fibers were IGF-IR− (based on visual examination; i.e., Fig. 3C). Many of the OMP+ axons penetrating into the DZ were IGF-IR−, but they may have been negative because of the lowered sensitivity of the IGF-IR antibody when using immunofluorescence. Because the frequency of IGF-IR+ fibers in the DZ is higher in peroxidase-labeled sections, we suspect that we are underestimating the co-localization between OMP and IGF-IR at this age.

At E19, like E18, there was a fairly complete overlap between OMP and IGF-IR labeling, especially in the ONL (Fig. 3D–F). Most of the protoglomeruli were OMP+/IGF-IR+ (Fig. 3, arrows). As at E18, some fibers positive for each label only were evident. The only major difference was seen in the relative intensities of each label. OMP labeling was intense throughout both the ONL and the protoglomeruli, while the intensity of IGF-IR labeling decreased in the protoglomeruli (Fig. 3D–E, arrows). This often resulted in the impression that some glomeruli were primarily OMP+, with little IGF-IR labeling. OMP+/IGF-IR+ fibers were observed penetrating the DZ, internal to the protoglomeruli (Fig. 3D–F). Fibers that were OMP+/IGF-IR− were also seen in this zone (Fig. 3D–F).

At P1, there was once again an almost complete co-localization of OMP and IGF-IR labeling in both the ONL and protoglomeruli (Fig. 3G–I). However, now it was common to find scattered glomeruli that were exclusively OMP+, with no distinguishable IGF-IR labeling (Fig. 3G–I, arrows).

In the adult, as mentioned previously, IGF-IR labeling was greatly reduced. Thus, although there were OMP+/IGF-IR+ glomeruli (Fig. 3J–L), the majority were OMP+/IGF-IR− (not shown). Most IGF-IR+ glomeruli were also labeled for OMP. Within OMP+/IGF-IR+ glomeruli, areas that were OMP+/IGF-IR+ were interdigitated with areas that were IGF-IR+ only (red) and areas that were OMP+ only (green) (Fig. 3J–L). We did not find OMP labeling in the smallest, most intensely labeled IGF-IR+ glomeruli.

Thus, in summary, the greatest overlap between OMP and IGF-IR labeling was seen at the earliest embryonic ages, although even this overlap was not complete. With increasing age of the animal, there was a decreasing amount of overlap between these two labels, which was consistent with decreasing labeling for IGR-IR in the OB. This developmental pattern was also consistent, in general, with the overlap between OMP and IGF-IR staining in ORN cell bodies in the OE (not shown).

Double-Labeling for Synaptophysin (SYN) and IGF-IR. At E18, SYN labeling was restricted to just a narrow band in the innermost portion of the ONL, with some extension of fibers into the DZ (Fig. 4A–C). In the transitional region between the ONL and the DZ, extensive co-localization between IGF-IR and SYN was observed (Fig. 4C). The fibers penetrating the DZ were IGF-IR+/SYN+ (Fig. 4C).

At E19, again, SYN labeling was absent from essentially all of the ONL (Fig. 4D–F). Thus the ONL was stained almost exclusively with IGF-IR. Now the protoglomeruli were intensely labeled with SYN (Fig. 4E–F). Within these structures, an almost complete co-localization of IGF-IR and SYN labeling was seen (Fig. 4D–F).

At P1, as at the previous stages, the ONL contained IGF-IR+ axons, but had no SYN labeling (Fig. 4G–I). However, within most of the glomeruli there was an extensive co-localization of IGF-IR and SYN labeling (Fig. 4G–I).

In the adult rat, the distribution of SYN labeling was very different from that found at the other stages. The majority of the glomeruli were positive for SYN labeling and negative for IGF-IR labeling (Fig. 4J–L). This was consistent with the fact that the majority of the glomeruli were IGF-IR− in the adult OB. Of the glomeruli that were IGF-IR+, most were also intensely positive for SYN labeling (Fig. 4J–L, center region). Within these glomeruli we found areas that were IGF-IR+ only interdigitated with areas that were SYN+ only (Fig. 4J–L). The SYN label seemed to be most strongly distributed around the periphery of the glomerulus, whereas IGF-IR labeling was more evenly distributed (Fig. 4J–L).

Thus there was overlap between SYN and IGF-IR labeling at all ages, with the greatest overlap seen in the areas most likely to contain developing synapses (the DZ margin, protoglomeruli, and then glomeruli). Fairly complete overlap was seen in the youngest animals with decreasing overlap with age.

Double-Labeling for GAP-43 and IGF-IR. At E18, there was extensive and almost complete co-localization between IGF-IR and GAP-43 labeling in both the ONL and the margin of the DZ (Fig. 5A–C), although occasional fibers could be identified as labeled singly with either antibody. In the OE (not shown), the overlap was not as complete, because many dendritic knobs and nerve bundles were IGF-IR+/GAP-43−. Thus the more complete overlap in the glomeruli suggests that perhaps adjacent axonal processes that were singly labeled appeared as double-labeled because of the resolution of our techniques.

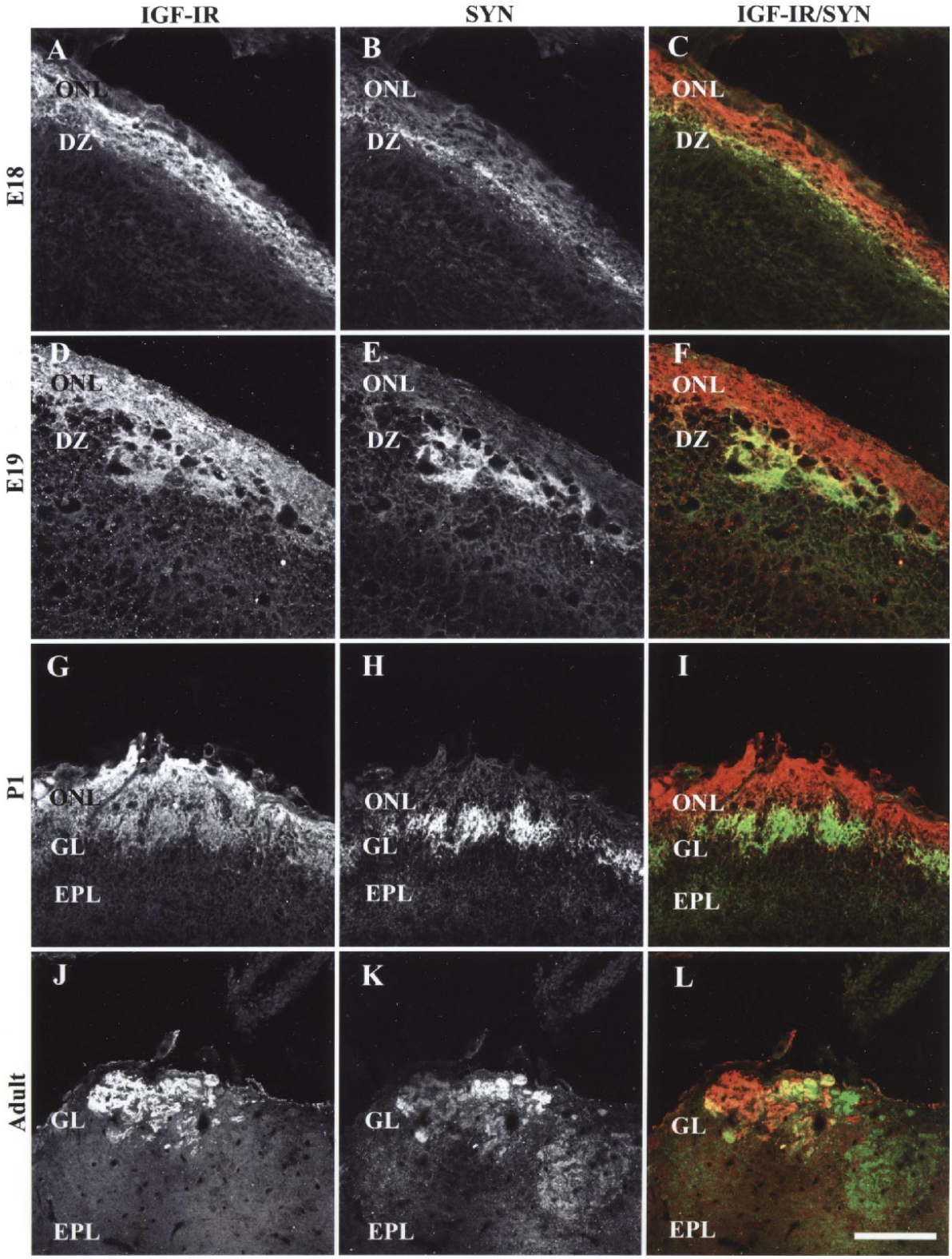

Fig. 4. Double immunofluorescence labeling: IGF-IR (red) and SYN (green). **A–C,** At E18, IGF-IR labeling was located throughout the ONL, while SYN labeling was observed only in the inner region of the ONL. Some co-localization (yellow) was observed. **D–F,** At E19, IGF-IR labeling was observed in the ONL and in some protoglomeruli, whereas SYN labeling was seen only in protoglomeruli. Co-localization was observed in the protoglomeruli (yellow in F). **G–I,** At P1 the labeling was quite similar to that seen at E18, with double-labeling seen in glomeruli. **J–L,** In the adult (postpubertal) rat, within IGF-IR+ glomeruli, we observed double-labeled areas (yellow in L), as well as areas that were positive for IGF-IR+ only (J, red in L) or SYN+ only (K, green in L). Scale bar for all = 100 μm. A color version of this figure can be viewed in the online version of the journal at http://www.kluweronline.com/issn/0364-3190.

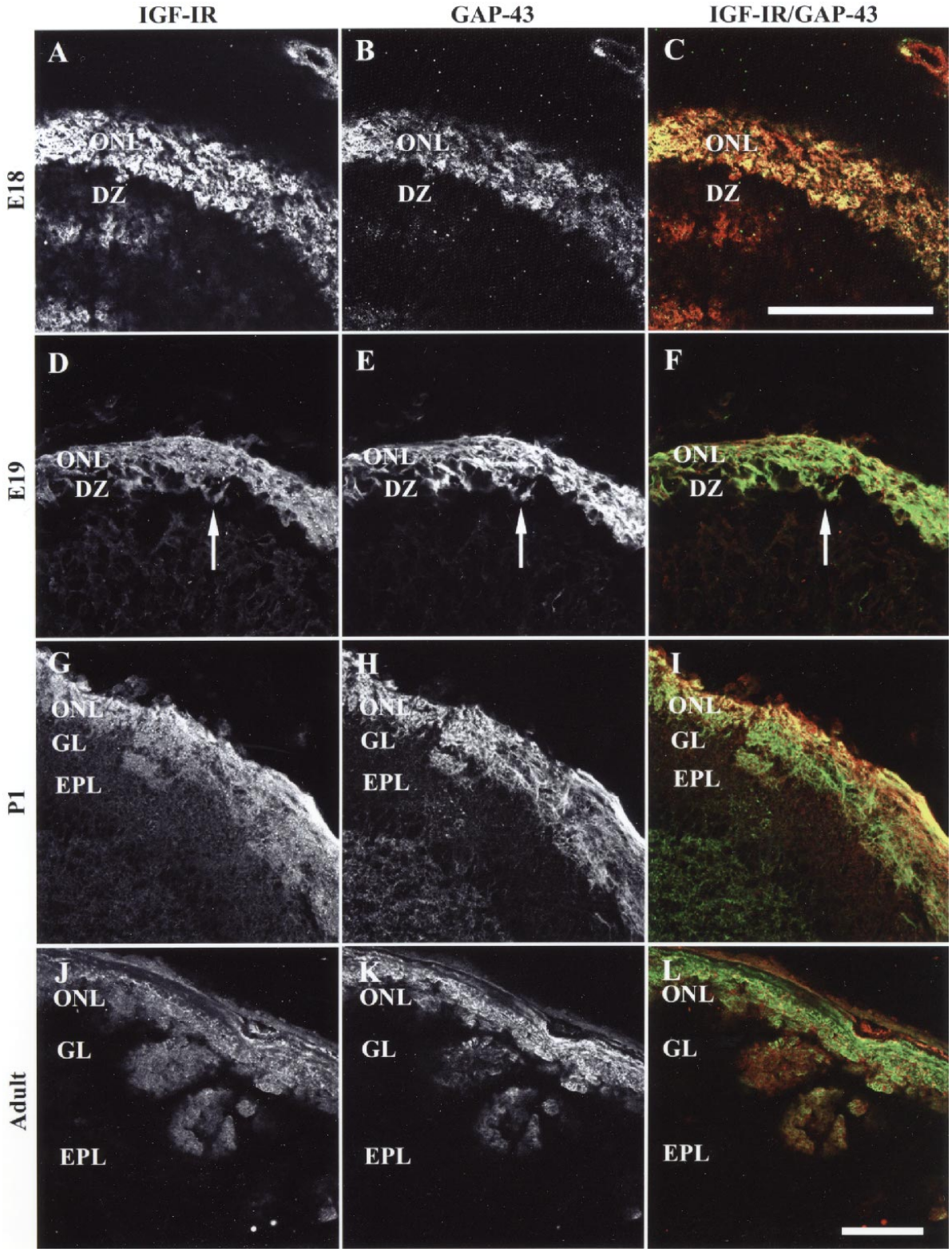

Fig. 5. Double immunofluorescence labeling: IGF-IR (red) and GAP-43 (green). **A–C,** At E18, IGF-IR and GAP-43 labeling were both distributed primarily in the ONL. Scale bar for A–C = 100 μm. **D–F,** At E19, double-labeling was observed both in the ONL and in protoglomeruli in the DZ (arrows). **G–I,** At P1, both IGF-IR and GAP-43 labeling were primarily in the ONL, with some double-labeled glomeruli in the GL (yellow). **J–L,** In the adult (postpubertal) rat, IGF-IR+ glomeruli contained areas that were double-labeled (yellow, L) and areas that showed IGF-IR (J, red in L) or GAP-43 (K, green in L) labeling alone. Scale bar for D–L = 100 μm. A color version of this figure can be viewed in the online version of the journal at http://www.kluweronline.com/issn/0364-3190.

At E19 and at P1, there was again an almost complete overlap between IGF-IR and GAP-43 labeling in both the ONL and the protoglomeruli (E19) (Fig. 5D–F) or the glomeruli (P1) (Fig. 5G–I).

In the adult rat, GAP-43 labeling was also found throughout the ONL, which meant that there was extensive overlap with IGF-IR labeling (Fig. 5J–L). GAP-43 labeling was found in glomeruli that were positive for IGF-IR (Fig. 5J–L), but it was also found in glomeruli that were negative for IGF-IR (not shown). Far more glomeruli were GAP-43+ than were IGF-IR+, demonstrating that not all immature ORN axons (GAP-43+) that reach the OB were IGF-IR+. Within double-labeled glomeruli, the pattern of GAP-43 labeling differed from that for IGF-IR. The GAP-43 labeling was most intense along the inner portion of the ONL and the portions of the glomeruli most proximal to the ONL (Fig. 5K, 5L), as has been described previously (34). In contrast, the IGF-IR labeling appeared to be more uniform throughout. Thus, different regions of the glomeruli showed different degrees of label co-localization and nonoverlap (Fig. 5L). The nonoverlapping labeling appeared as punctuate areas of fibers singly labeled for either GAP-43 (most often seen peripherally and proximally within the glomerulus) or IGF-IR (more often seen distally) interdigitated with double-labeled areas (Fig. 5J–L). The small, intensely labeled IGF-IR+ glomeruli were also usually labeled for GAP-43.

Thus, as for OMP labeling, the overlap between GAP-43 and IGF-IR labeling was greatest in the embryonic animals and was reduced in adults, suggesting that only a subset of immature ORN axons (GAP-43+) that reach the OB are also IGF-IR+. Overlap with GAP-43 is consistent with the fact that IGF-IR labeling has been found previously in immature ORNs in the epithelium (25).

DISCUSSION

This study shows that the highest levels of IGF-IR immunoreactivity occurred in the right areas and during the right times for IGF-I and its receptor to play a role in ORN axon ingrowth into, ORN synapse formation in or glomerular formation in the OB.

What Might Be the Role of IGF-I in the Brain? Previous studies of the patterns of IGF-I and IGF-IR mRNA expression during CNS development suggested that IGF-I plays a role in axon outgrowth and/or maturation of synaptic connections (45). Whereas IGF-IR mRNA is expressed at low levels uniformly throughout the CNS, which would be consistent with a general nutritive and survival support role for most neural cells, a more restricted distribution is seen for cells expressing high levels of IGF-I and IGF-IR mRNA (45). High levels of expression are restricted to large projection neurons in the cerebellum, thalamus, retina, OB, and hippocampus, and in target regions of these neurons. And except for the OB, where expression continues into adulthood, expression is primarily transient, occurring at a time after neurogenesis when axons reach their targets and complete synaptogenesis (45). Thus, IGF-I was thought to play a role in the establishment of axonal connections in local circuits, notably sensory and cerebellar pathways (45).

More recently, Bondy and colleagues have advanced the hypothesis that IGF-I regulates neuronal metabolism of glucose during development and plasticity (18). Because the brain consumes greater energy than is explained by its relative size and weight and does not appear to use insulin like peripheral tissues, they suggest that, instead, the brain may use IGF-I to regulate and facilitate brain glucose metabolism. They then provided strong evidence that IGF-I mediates anabolic cellular pathways that are consistent with an insulin-like effect on neurons (18). This role is consistent with the CNS studies, because expression is limited to very large neurons and time periods of axonal outgrowth and synapse formation, processes that require significant cellular energy.

IGF-IR+ Fibers Are in the Right Time and Place in the OB to Be Involved in Glomerular Formation and/or Synaptogenesis. Involvement in glomerular formation and/or synaptogenesis in the OB might require higher energy on the part of the ORN, thus requiring greater activity of IGF-I. Our data suggest that the IGF-IR–labeled fibers were at the right time and place to be involved in these processes. First, high levels of IGF-IR were present in the ONL, DZ, protoglomeruli, and GL, all of which are major sites of axon ingrowth, synapse formation, and glomerular formation during OB development. ORN axons grow into and surround the OB around E13-14 in the rat (37,46,47), and synapse formation with OB dendrites is initiated when ORN axons penetrate the presumptive glomerular area (the DZ), around E14–15 in the mouse (equivalent to E16–17 in the rat) (48,49). Glomerular formation is initiated with the appearance of protoglomeruli at the edge of the DZ, around E18 in the rat, followed by true glomeruli and the GL just after birth, again in the rat (31,32). We observed the most extensive IGF-IR labeling in the same OB layers during these perinatal time periods.

A second observation was that IGF-IR labeling in the OB overlapped extensively during the perinatal period with labeling for SYN, which indicates that IGF-IR+ fibers were in the appropriate location to be associated with developing synapses.

A third observation was that IGF-IR+ fibers were double-labeled with both GAP-43 and OMP, suggesting that IGF-IR might be expressed by both immature and mature ORNs, perhaps at critical times of formation or stabilization of synapses. We previously demonstrated IGF-IR labeling in a subset of immature ORNs in the newborn and adult rat OE (25). We have more recently determined, by double-labeling for IGF-IR and the neural cell adhesion molecule (NCAM) that only a subset of immature ORNs is IGF-IR+. And an even smaller subset of mature, OMP+ ORNs is IGF-IR+ (Pixley, unpublished data). This labeling is consistent with our OB labeling in P1 and adults, as reported here. One possible hypothesis for these data is that ORNs express IGF-IRs in a time-dependent manner, that is, beginning late in ORN immaturity, at about the time that ORN axons enter the glomeruli. And the ORNs would then have to cease expression just after completing maturation, which involves morphological changes and initiation of OMP expression. What triggers or stimulates maturation of ORNs is not known. This time-dependent expression of IGF-IRs would allow the ORNs to take advantage of the unusually high production of IGF-I that is characteristic of the intrinsic OB neurons that are the targets of ORNs (19,45,50–52). Thus the ORNs might therefore use IGF-I in the possibly energy-demanding processes of either maturation, or synapse formation and stabilization. A second possibility is that IGF-IRs are highly expressed in a subset of ORNs, regardless of their maturation state. If so, we would speculate that this subset might require higher levels of metabolic energy. A third possibility is that a subset of ORNs expresses high levels of IGF-IRs, but only at a certain time in their lifespan. All we can say at present is that the IGF-IR expression pattern in ORNs in the OB is consistent with an involvement in either synaptogenesis or glomerular formation, which would support a role for IGF-I in energy-demanding processes.

In summary, our data are consistent with a hypothesis that IGF-I and the IGF-IR are involved in some aspect of ORN axonal growth, synapse formation and/or glomerular formation in the OB. All of these processes are energy demanding, so the speculated role of IGF-I would be to enhance the energy utilization of ORNs during establishment of either position or synapses.

Is Our Immunolabeling Consistent with Previous Studies of IGF Components? Our immunolabeling is consistent with, but may be less sensitive than, previous labeling for the production and presence of IGF-IR. Autoradiographic studies of IGF-I binding localized the highest levels of putative IGF-IRs in the ONL and Gl in the adult, with uniform labeling, and lower labeling in the EPL and internal plexiform layers (45,53–55). Our highest labeling was also in the ONL and GL, but we saw incomplete labeling in the adult and we did not observe labeling in any other OB layer at any time. The differences may be due to the fact that, in autoradiography, cellular localization is sacrificed to gain increased sensitivity while in antibody staining, cellular detail and localization may be gained at the expense of sensitivity. Another possibility is that with autoradiography, despite attempts to the contrary, binding of radioactive IGF-I to its many binding proteins may not have been completely eliminated. The IGF-I binding proteins (IGFBPs) are abundantly expressed in the OB (56).

In situ hybridization studies in the OB show IGF-IR mRNA expressed in granular, mitral, and tufted cells, with lower levels in the GL (45,51,55,57–59). We did not observe any labeling of OB neurons, but the differences could readily be due to a lower sensitivity with the antibody. The in situ studies did not examine the OE, so the relative level of IGF-IR mRNA expression in ORN cell bodies versus OB neurons is not known. It is also possible that the differences between immunostaining and in situ results are due to the production of mRNA without translation into protein, or rapid transport of the protein to specific areas of the cells, such as the apical dendrites of the mitral cells. In regard to the latter speculation, our IGF-IR+ labeling in glomeruli did not appear to be labeling of mitral or tufted cell processes, although we cannot rule that out at present. In summary, our results suggest that this IGF-IR antibody only detects cells expressing the highest levels of IGF-IR protein, which appear to be a subset of ORNs.

Small, Intensely IGF-IR+ Glomeruli. We observed small, intensely IGF-IR+ glomeruli-like regions in the transition zone between the GL and EPL. They do not appear to be off-center slices of larger positive glomeruli because of the distinctive difference in staining (see Figs.) and because of observations in serially sectioned tissues (not shown). The fact that these areas showed no OMP double-labeling, but did show double-labeling with GAP-43 and SYN, supports the idea that these fibers are immature ORNs initiating synaptogenesis. These areas are unlikely to be newly forming glomeruli, because previous reports

have suggested that there are no new glomeruli formed in the adult rat (60). However, increases in glomerular size and number have been reported in the adult mouse (61), so one speculation is that these sets of IGF-IR+ fibers are newly forming glomerular areas that eventually become incorporated into neighboring glomeruli.

Despite the previously mentioned morphological study in the mouse, functional studies in young adult rats argue against expansion of glomeruli. In young rats, glomerular function and size expand if there is an increase in odor exposure during the first weeks after birth (62–65). However, a critical period was observed for alterations in glomerular function; changes did not occur when the odorant exposure occurred after the first few weeks of life (66). Thus, presumably, there are fewer or no glomerular changes in adults. Although it might be optimal to revisit this issue combining odorant exposure, functional measures and IGF-IR staining, the behavioral and morphometric analyses are quite complex (64) and the IGF-IR+ glomeruli are few in number, so subtle changes occurring in adults might be missed.

Other laboratories have described unusually small glomeruli in the OB. Kosaka et al. described small glomeruli, termed nidi, in the shrew that label for both glutamic acid decarboxylase and calbindin (67, 68). However, they differ significantly from our small IGF-IR+ glomeruli, in that the nidi are more numerous in the adult, forming a distinctive layer throughout the OB, and the nidi contain only processes of OB neurons, not ORN axons (68). Greer and colleagues described small glomeruli labeled with the lectin, UEA that contained ORN axons that were OMP+ but NCAM− and appeared to be a subset of mature ORNs (69). In contrast, our small IGF-IR+ glomeruli were OMP− and GAP-43+, which suggests that they contain immature ORN axons. Thus, although more extensive analysis remains to be done, including double-labeling with UEA lectin, we appear to be describing a new set of glomerular-like structures.

IGF-IR+ Fibers Penetrated the EPL Layer in Adult OBs. Another unusual observation was that IGF-IR+ fibers extended into the EPL in adult rats. Axons of ORN that penetrate the EPL have been observed in embryonic and perinatal rodents (70,71). This was thought to indicate that the laminar targeting of ORN axons in the OB is imprecise initially, that is, around P1.5 (71). However, no ORN axons penetrating deep to the GL were found in adults (70,71). Here we saw immature (OMP−), IGF-IR+ fibers (presumably ORN axons) extending deep to the GL in adult animals as well as in younger animals. It is tempting to speculate that the IGF-IR+ fibers that we saw extending deep to the GL in both adults and younger animals have a function in plasticity in the OB, perhaps in restructuring glomeruli. Other previous studies have described a population of "almost mature" neurons in the OB that are unable to find synaptic space and determined that these represent the bulk of turnover of ORNs that occurs continuously (72,73). Thus these extraneous, deep IGF-IR+ fibers, as well as the small glomeruli, might be fibers that have not yet and may never find an appropriate place in a glomerulus, and are destined to be rapidly lost.

Significance of the Labeling of a Subset of ORN Axons in the Adult. As stated above, hypotheses to be considered are whether IGF-IRs are expressed during one time period in the life of all ORNs, or by only a subset of ORNs. A key factor in sorting this out may be to determine if the IGF-IR+ glomeruli in the adult are randomly located or appear in specific patterns from animal to animal. If IGF-IR labeling were stage-specific and in all ORNs, then the glomeruli would presumably be randomly located, because dividing cells in the OE are randomly distributed (74). In our studies of IGF-IR+ neurons in the OE, observations of the septum showed randomly scattered neurons that were not localized to zones (Pixley, unpublished results), as is observed with olfactory receptor genes (26,75). If the glomeruli are not randomly located, then the IGF-IR+ ORNs are more likely to be a subset, perhaps with unusual energy requirements. Because the current work suggested a nonrandom distribution (i.e., we consistently found more labeled glomeruli in the posterior rather than anterior OB in adults), work is currently underway in our laboratory to map (and quantify) the interanimal distribution patterns of IGF-IR+ glomeruli.

Compartmentalization within Glomeruli. As has been found for other antigens, we observed a compartmentalized distribution of IGF-IR within adult glomeruli. Previous observations of compartmentalized glomerular distributions of GAP-43, SYN, and OMP led to the suggestion that axo- and dendro-dendritic circuits are segregated into separate compartments (32,34). In our double-labeling studies, we saw a fairly extensive co-localization of IGF-IR with OMP, SYN, and GAP-43 through development until we examined adult rats. There we saw heterogeneous labeling for each marker. Single- as well as double-labeling was seen for each antibody marker. Most interesting was the discordance between OMP and IGF-IR staining in glomeruli, because it suggests that different types of ORN endings, perhaps based on age or energy

utilization, could be compartmentalized within the glomerulus.

IGF-I Could Affect Axon Targeting Instead of or in Addition to Neuronal Glucose Metabolism. Targeting to glomeruli by ORN axons undoubtedly depends on a series of specific cell surface molecules, trophic factors and/or tropic factors (28,31,76). Based on our results shown here, IGF-I could be a candidate for a bulb-derived trophic or tropic factor, instead of, or in addition to, being involved in neuronal metabolism. Although IGF-I has not been reported to have intrinsic tropic actions, it is associated with a family of extracellular binding proteins, IGFBPs, that regulate its activity in a tissue and age-specific manner (77,78). Many IGFBPs are found in the outer layers of the rodent OB (51,56,79), and they could bind IGF-I extracellularly and present it to ORN axons locally, or by diffusion of soluble IGFBPs, farther away (78). This could make IGF-I a spatial cue, guiding ORN axonal routing. Alternatively, IGF-I might influence axonal targeting by altering the extracellular matrix, because IGF-I can stimulate extracellular matrix production (36,80), and extracellular matrix molecules have been implicated in guidance of ORN axons (35,37,81). Thus, IGF-I could modify axonal outgrowth and glomerular formation in ways other than by influencing neuronal glucose metabolism.

SUMMARY

In summary, the IGF-IR is expressed on a subset of predominantly immature ORN axons in the embryonic, postnatal and adult rat OB. The spatiotemporal expression of the IGF-IR immunoreactivity in the OB and co-labeling with GAP-43, OMP and SYN support a role for IGF-IR, and therefore the IGF-I system, in the development of glomeruli and/or synapse formation in the OB. This may occur by boosting the metabolism of glucose by ORNs during periods of axon contact with target neurons and synapse formation. Further studies of the IGF-I system may elucidate mechanisms involved in regeneration of ORNs, maturation of glomeruli and/or formation and plasticity of synaptic contacts within the olfactory system.

ACKNOWLEDGMENTS

The authors are very grateful to Dr. Nancy Koster for her kind help with the confocal microscopy. This work was supported by the following grants and funding: NIH DC00347 (SP), CONICET postdoctoral fellowship (CF), Fullbright postdoctoral fellowship (CF), and NIH DC03545 (ML).

REFERENCES

1. Hansson, H. A., Nilsson, A., Isgaard, J., Billig, H., Isaksson, O., Skottner, A., Andersson, I. K., and Rozell, B. 1988. Immunohistochemical localization of insulin-like growth factor I in the adult rat. Histochem. 89:403–410.
2. DiCicco-Bloom, E. and Black, I. B. 1988. Insulin growth factors regulate the mitotic cycle in cultured rat sympathetic neuroblasts. Proc. Natl. Acad. Sci. U.S.A. 85:4066–4070.
3. Zackenfels, K., Oppenheim, R. W., and Rohrer, H. 1995. Evidence for an important role of IGF-I and IGF-II for the early development of chick sympathetic neurons. Neuron. 14:731–741.
4. Lindholm, D., Carrol, P., Tzimagiorgis, G., and Thoenen, H. 1996. Autocrine-paracrine regulation of hippocampal neuron survival by IGF-I and neurotrophins BDNF, NT-3 and NT-4. Eur. J. Neurosci. 8:1452–1460.
5. Recio-Pinto, E., Rechler, M. M., and Ishii, D. N. 1986. Effects of insulin, insulin-like growth factor-II, and nerve growth factor on neurite formation and survival in cultured sympathetic and sensory neurons. J. Neurosci. 6:1211–1219.
6. Torres-Aleman, I., Pons, S., and Arevalo, M. A. 1994. The insulin-like growth factor I system in the rat cerebellum: Developmental regulation and role in neuronal survival and differentiation. J. Neurosci. Res. 39:117–126.
7. Cheng, B. and Mattson, M. P. 1992. IGF-I and IGF-II protect cultured hippocampal and septal neurons against calcium-mediated hypoglycemic damage. J. Neurosci. 12:1558–1566.
8. D'Mello, S. R., Galli, C., Ciotti, T., and Calissano, P. 1993. Induction of apoptosis in cerebellar granule neuros by low potassium: Inhibition of death by insulin-like growth factor I and cAMP. Proc. Natl. Acad. Sci. U.S.A. 90:10989–10993.
9. Miller, T. M. and Johnson, E. M. J. 1996. Metabolic and genetic analyses of apoptosis in potassium/serum-deprived rat cerebellar granule cells. J. Neurosci. 16:7487–7495.
10. Fernyhough, P., Mill, J. F., Roberts, J. L., and Ishii, D. N. 1989. Stabilization of tubulin mRNAs by insulin and insulin-like growth factor I during neurite formation. Mol. Brain Res. 6:109–120.
11. Kessler, J. A., Spray, D. C., Saez, J. C., and Bennett, M. V. 1984. Determination of synaptic phenotype: Insulin and cAMP independently initiate development of electronic coupling between cultured sympathetic neurons. Proc. Natl. Acad. Sci. U.S.A. 81:6235–6239.
12. Knusel, B. and Hefti, F. 1991. Trophic actions of IGF-I, IGF-II and insulin on cholinergic and dopaminergic brian neurons: in Molecular Biology and Physiology of Insulin and Insulin-Like Growth Factors (Raizada, M. K. and LeRoith, D. eds), Plenum Press, New York.
13. Wolinsky, E. J., Patterson, P. H., and Willard, A. L. 1985. Insulin promotes electrical coupling between cultured sympathetic neurons. J. Neurosci. 5:1675–1679.
14. Xue, Z. G., Le Douarin, N. M., and Smith, J. 1988. Insulin and insulin-like growth factor-I can trigger the differentiation of catecholaminergic precursors in cultures of dorsal root ganglia. Cell Diff. Dev. 25:1–10.
15. Baker, N. L., Carlo Russo, V., Bernard, O., D'Ercole, A. J., and Werther, G. A. 1999. Interactions between bcl-2 and the IGF system control apoptosis in the developing mouse brain. Dev. Brain Res. 118:109–118.
16. Werther, G. A., Russo, V., Baker, N., and Butler, G. 1998. The role of the insulin-like growth factor system in the developing brain. Horm. Res. 49:37–40.
17. Åberg, M. A., Åberg, N. D., Hedbäcker, H., Oscarsson, J., and Eriksson, P. S. 2000. Peripheral infusion of IGF-I selectively induces neurogenesis in the adult rat hippocampus. J. Neuroscience 20:2896–2903.

18. Cheng, C. M., Reinhardt, R. R., Lee, W. H., Joncas, G., Patel, S. C., and Bondy, C. A. 2000. Insulin-like growth factor 1 regulates developing brain glucose metabolism. Proc. Natl. Acad. Sci. U.S.A. 97:10236–10241.
19. Bondy, C. A. 1991. Transient IGF-I gene expression during the maturation of functionally related central projection neurons. J. Neurosci. 11:3442–3455.
20. LeRoith, D., Werner, H., Faria, T. N., Kato, H., Adamo, M., and Roberts, C. T., Jr. 1993. Insulin-like growth factor receptors: Implications for nervous system function. Ann. N.Y. Acad. Sci. 692:22–32.
21. Farbman, A. I. 1990. Olfactory neurogenesis: Genetic or environmental controls? TINS. 13:362–365.
22. Graziadei, P. P. C. and Monti-Graziadei, G. A. 1978. Continuous nerve cell renewal in the olfactory system. Pages 55–84, in Jacobson, M. (eds), Handbook of Sensory Physiology. Springer-Verlag, New York.
23. Schwob, J. E., Szumowski, K. E. M., and Stasky, A. A. 1992. Olfactory sensory neurons are trophically dependent on the olfactory bulb for their prolonged survival. J. Neurosci. 12: 3896–3919.
24. McEntire, J. K. and Pixley, S. K. 2000. Olfactory receptor neurons in partially purified epithelial cell cultures: Comparison of techniques for partial purification and identification of insulin as an important survival factor. Chem. Senses. 25:93–101.
25. Pixley, S. K., Dangoria, N. S., Odoms, K. K., and Hastings, L. 1998. Effects of insulin-like growth factor 1 on olfactory neurogenesis in vivo and in vitro. Ann. N.Y. Acad. Sci. 855: 244–247.
26. Buck, L. B. and Axel, R. 1991. A novel multigene family may encode odorant receptors: A molecular basis for odor recognition. Cell. 65:175–187.
27. Buck, L. B. 1996. Information coding in the vertebrate olfactory system. Annu. Rev. Neurosci. 19:517–544.
28. Mombaerts, P., Wang, F., Dulac, C., Chao, S. K., Nemes, A., Mendelsohn, M., Edmondson, J., and Axel, R. 1996. Visualizing an olfactory sensory map. Cell. 87:675–686.
29. Johnson, B. A., Woo, C. C., and Leon, M. 1998. Spatial coding of odorant features in the glomerular layer of the rat olfactory bulb. J. Comp. Neurol. 393:457–471.
30. Johnson, B. A. and Leon, M. 2000. Modular representations of odorants in the glomerular layer of the rat olfactory bulb and the effects of stimulus concentration. J. Comp. Neurol. 422: 496–509.
31. Valverde, F., Santacana, M., and Heredia, M. 1992. Formation of an olfactory glomerulus: Morphological aspects of development and organization. Neuroscience 49:255–275.
32. Treloar, H. B., Purcell, A. L., and Greer, C. A. 1999. Glomerular formation in the developing rat olfactory bulb. J. Comp. Neurol. 413:289–304.
33. Monti Graziadei, G. A., Stanley, R. S., and Graziadei, P. P. C. 1980. The olfactory marker protein in the olfactory system of the mouse during development. Neuroscience 5:1239–1252.
34. Kim, H. and Greer, C. A. 2000. The emergence of compartmental organization in olfactory bulb glomeruli during postnatal development. J. Comp. Neurol. 422:297–311.
35. Gonzalez, M. D., Malemud, C. J., and Silver, J. 1993. Role of astroglial extracellular matrix in the formation of rat olfactory bulb glomeruli. Exp. Neurol. 123:91–105.
36. Taipale, J. and Keski-Oja, J. 1997. Growth factors in the extracellular matrix. FASEB J. 11:51–59.
37. Treloar, H. B., Nurcombe, V., and Key, B. 1996. Expression of extracellular matrix molecules in the embryonic rat olfactory pathway. J. Neurobiol. 31:41–55.
38. Dowsing, B., Puche, A., Hearn, C., and Key, B. 1997. Presence of novel N-CAM glycoforms in the rat olfactory system. J. Neurobiol. 32:659–670.
39. Puche, A. C. and Key, B. 1995. Identification of cells expressing galectin-1, a galactose-binding receptor, in the rat olfactory system. J. Comp. Neurol. 357:513–523.
40. Puche, A. C. and Key, B. 1996. *N*-Acetyl-lactosamine in the rat olfactory system: Expression and potential role in neurite growth. J. Comp. Neurol. 364:267–278.
41. Margolis, F. 1980. A marker protein for the olfactory chemoreceptor neuron. Pages 59–84, in Bradshaw, R. A. and Schneider, D. (eds), Proteins of the Nervous System. Raven, New York.
42. Verhaagen, J., Oestreicher, A. B., Gispen, W. H., and Margolis, F. L. 1989. The expression of the growth associated protein B50/GAP43 in the olfactory system of neonatal and adult rats. J. Neurosci. 9:683–691.
43. Jahn, R. Schiebler, W., Ouimet, C., and Greengard, P. 1985. A 38,000-dalton membrane protein (p38) present in synaptic vesicles. Proc. Natl. Acad. Sci. U.S.A. 82:4137–4141.
44. Harlow, E. and Lane, D. 1988. Gelvatol. Page 418, in Harlow, E. and Lane, D. (eds), Antibodies: A Laboratory Manual, Cold Spring Harbor Laboratory, Cold Spring Harbor, New York.
45. Bondy, C. A., Werner, H., Roberts, C. T. J., and LeRoith, D. 1992. Cellular pattern of type-I insulin-like growth factor receptor gene expression during maturation of the rat brain: Comparison with insulin-like growth factors I and II. Neuroscience 46:909–923.
46. Gong, Q. and Shipley, M. T. 1995. Evidence that pioneer olfactory axons regulate telencephalon cell cycle kinetics to induce the formation of the olfactory bulb. Neuron. 14:91–101.
47. Gong, Q. and Shipley, M. T. 1996. Expression of extracellular matrix molecules and cell surface molecules in the olfactory nerve pathway during early development. J. Comp. Neurol. 366:1–14.
48. Hinds, J. W. 1972. Early neuron differentiation in the mouse olfactory bulb. II. Electron microscopy. J. Comp. Neurol. 146: 253–276.
49. Hinds, J. W. and Hinds, P. L. 1976. Synapse formation in the mouse olfactory bulb. I. Quantitative studies. J. Comp. Neurol. 169:15–40.
50. Bohannon, N. J., Corp, E. S., Wilcox, B. J., Figlewicz, D. P., Dorsa, D. M., and Baskin, D. G. 1988. Localization of binding sites for IGF-I in the rat brain by quantitative autoradiography. Brain Res. 444:205–213.
51. Bondy, C. A. and Lee, W. H. 1993. Correlation between insulin-like growth factor (IGF)-binding protein 5 and IGF-I gene expression during brain development. J. Neurosci. 13: 5092–5104.
52. Bondy, C. A. and Lee, W. H. 1993. Patterns of insulin-like growth factor and IGF receptor gene expression in the brain: Functional implications. Ann. N.Y. Acad. Sci. 692:33–43.
53. Lesniak, M. A., Hill, J. M., Kiess, W., Rojeski, M. Pert, C. B., and Roth, J. 1988. Receptors for insulin-like growth factors I and II: Autoradiographic localization in rat brain and comparison to receptors for insulin. Endocrinology 123:2089–2099.
54. Werther, G. A., Hogg, A., Oldfield, B. J., McKinley, M. J., Figdor, R., Allen, A. M., and Mendelsohn, F. A. 1987. Localization and characterization of insulin receptors in rat brain and pituitary gland using in vitro autoradiography and computerized densitometry. Endocrinology 121:1562–1570.
55. Werther, G. A., Abate, M., Hogg, A., Cheesman, H., Oldfield, B., Hards, D., Hudson, P., Power, B., Freed, K., and Herington, A. C. 1990. Localization of insulin-like growth factor-I mRNA in rat brain by in situ hybridization: Relationship to IGF-I receptors. Mol. Endocrinol. 4:773–778.
56. Russo, V. C., Edmondson, S. R., Mercuri, F. A., Buchanan, C. R., and Werther, G. A. 1994. Identification, localization, and regulation of insulin-like growth factor binding proteins and their messenger ribonucleic acids in the newborn rat olfactory bulb. Endocrinology 135:1437–1446.
57. Bondy, C. A., Werner, H., Roberts, C. T. J., and LeRoith, D. 1990. Cellular pattern of insulin-like growth factor-I (IGF-I) and type I IGF receptor gene expression in early organogenesis: Comparison with IGF-II gene expression. Mol. Endocrinol. 4:1386–1398.
58. Marks, J. L., Porte, D. J., and Baskin, D. G. 1991. Localization

of type I insulin-like growth factor receptor messenger RNA in the adult rat brain by in situ hybridization. Mol. Endocrinol. 5:1158–1168.
59. Marks, J. L., King, M. G., and Baskin, D. G. 1991. Localization of insulin and type I IGF receptors in rat brain by in vitro autoradiography and in situ hybridization. Pages 459–470, in Raizada, M. K. and LeRoith, D. (eds), Molecular Biology and Physiology of Insulin and Insulin-Like Growth Factors. Plenum Press, New York.
60. Meisami, E. and Sendera, T. J. 1993. Morphometry of rat olfactory bulbs stained for cytochrome oxidase reveals that the entire population of glomeruli forms early in the neonatal period. Brain Res. Dev. Brain Res. 71:253–257.
61. Pomeroy, S. L., LaMantia, A. S., and Purves, D. 1990. Postnatal construction of neural circuitry in the mouse olfactory bulb. J. Neurosci. 10:1952–1966.
62. Coopersmith, R. and Leon, M. 1984. Enhanced neural response to familiar olfactory cues. Science. 225:849–851.
63. Johnson, B. A., Woo, C. C., Duong, H., Nguyen, V., and Leon, M. 1995. A learned odor evokes an enhanced Fos-like glomerular response in the olfactory bulb of young rats. Brain Res. 699:192–200.
64. Woo, C. C., Coopersmith, R., and Leon, M. 1987. Localized changes in olfactory bulb morphology associated with early olfactory learning. J. Comp. Neurol. 263:113–125.
65. Woo, C. C. and Leon, M. 1991. Increase in a focal population of juxtaglomerular cells in the olfactory bulb associated with early learning. J. Comp. Neurol. 305:49–56.
66. Woo, C. C. and Leon, M. 1987. Sensitive period for neural and behavioral response development to learned odors. Brain Res. 433:309–313.
67. Kosaka, K. and Kosaka, T. 1999. Distinctive neuronal organization of the olfactory bulb of the laboratory shrew. Neuroreport 10:267–273.
68. Kosaka, K. and Kosaka, T. 2001. Nidus and tasseled cell: Distinctive neuronal organization of the main olfactory bulb of the laboratory musk shrew (*Suncus murinus*). J. Comp. Neurol. 430:542–561.
69. Lipscomb, B., Treloar, H., and Greer, C. 2002. Novel microglomerular structures in the olfactory bulb of mice. J. Neurosci. 22:766–774.
70. Santacana, M., Heredea, M., and Valverde, F. 1992. Transient pattern of exuberant projections of olfactory axons during development in the rat. Dev. Brain Res. 70:213–222.
71. Tenne-Brown, J. and Key, B. 1999. Errors in lamina growth of primary olfactory axons in the rat and mouse olfactory bulb. J. Comp. Neurol. 410:20–30.
72. Hinds, J. W., Hinds, P. L., and McNelly, N. A. 1984. An autoradiographic study of the mouse olfactory epithelium: Evidence for long-lived receptors. Anal. Rec. 210:375–383.
73. Mackay-Sim, A. and Kittel, P. W. 1991. Cell dynamics in the adult mouse olfactory epithelium: A quantitative autoradiographic study. J. Neurosci. 11:979–984.
74. Weiler, E. and Farbman, A. I. 1997. Proliferation in the rat olfactory epithelium: Age-dependent changes. J. Neurosci. 17: 3610–3622.
75. Vassar, R., Ngai, J., and Axel, R. 1993. Spatial segregation of odorant receptor expression in the mammalian olfactory epithelium. Cell. 74:309–318.
76. Klenoff, J. R. and Greer, C. A. 1998. Postnatal development of olfactory receptor cell axonal arbors. J. Comp. Neurol. 390: 256–267.
77. Kelley, K. M., Oh, Y., Gargosky, S. E., Gucev, Z., Matsumoto, T., Hwa, V., Ng, L., Simpson, D. M., and Rosenfeld, R. G. 1996. Insulin-like growth factor-binding proteins (IGFBPs) and their regulatory dynamics. Int. J. Biochem. Cell Biol. 28:619–637.
78. Sara, V. R. and Hall, K. 1990. Insulin-like growth factors and their binding proteins. Physiol. Rev. 70:591–614.
79. Lee, W.-H., Michels, K. M., and Bondy, C. A. 1993. Localization of insulin-like growth factor binding protein-2 messenger RNA during postnatal brain development: Correlation with insulin-like growth factors I and II. Neuroscience 53:251–265.
80. Pricci, F., Pugliese, G., Romano, G., Romeo, G., Locuratolo, N., Pugliese, F., Mene, P., Galli, G., Casini, A., Rotella, C. M., and Di Mario, U. 1996. Insulin-like growth factors I and II stimulate extracellular matrix production in human glomerular mesangial cells: Comparison with transforming growth factor-beta. Endocrinology 137:879–885.
81. Crandall, J. E., Dibble, C., Butler, D., Pays, L., Ahmad, N., Kostek, C., Puschel, A. W., and Schwarting, G. A. 2000. Patterning of olfactory sensory connections is mediated by extracellular matrix proteins in the nerve layer of the olfactory bulb. J. Neurobiol. 45:195–206.